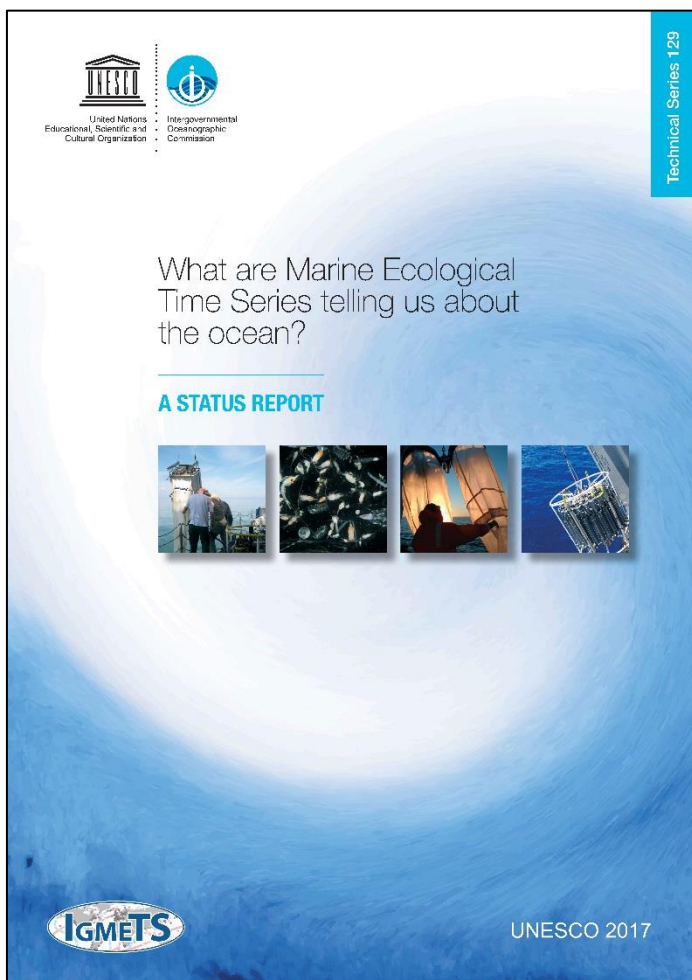


# *What are Marine Ecological Time Series telling us about the ocean? A status report*

[ Individual Chapter (PDF) download ]

The full report (all chapters and Annex) is available online at:

<http://igmets.net/report>



**Chapter 01:** New light for ship-based time series (Introduction)

**Chapter 02:** Methods & Visualizations

**Chapter 03:** Arctic Ocean

**Chapter 04:** North Atlantic

**Chapter 05:** South Atlantic

**Chapter 06:** Southern Ocean

**Chapter 07:** Indian Ocean

**Chapter 08:** South Pacific

**Chapter 09:** North Pacific

**Chapter 10:** Global Overview

**Annex:** Directory of Time-series Programmes

This page intentionally left blank  
to preserve pagination in double-sided (booklet) printing

# 5 South Atlantic Ocean

Frank E. Muller-Karger, Alberto Piola, Hans M. Verheye, Todd D. O'Brien, and Laura Lorenzoni

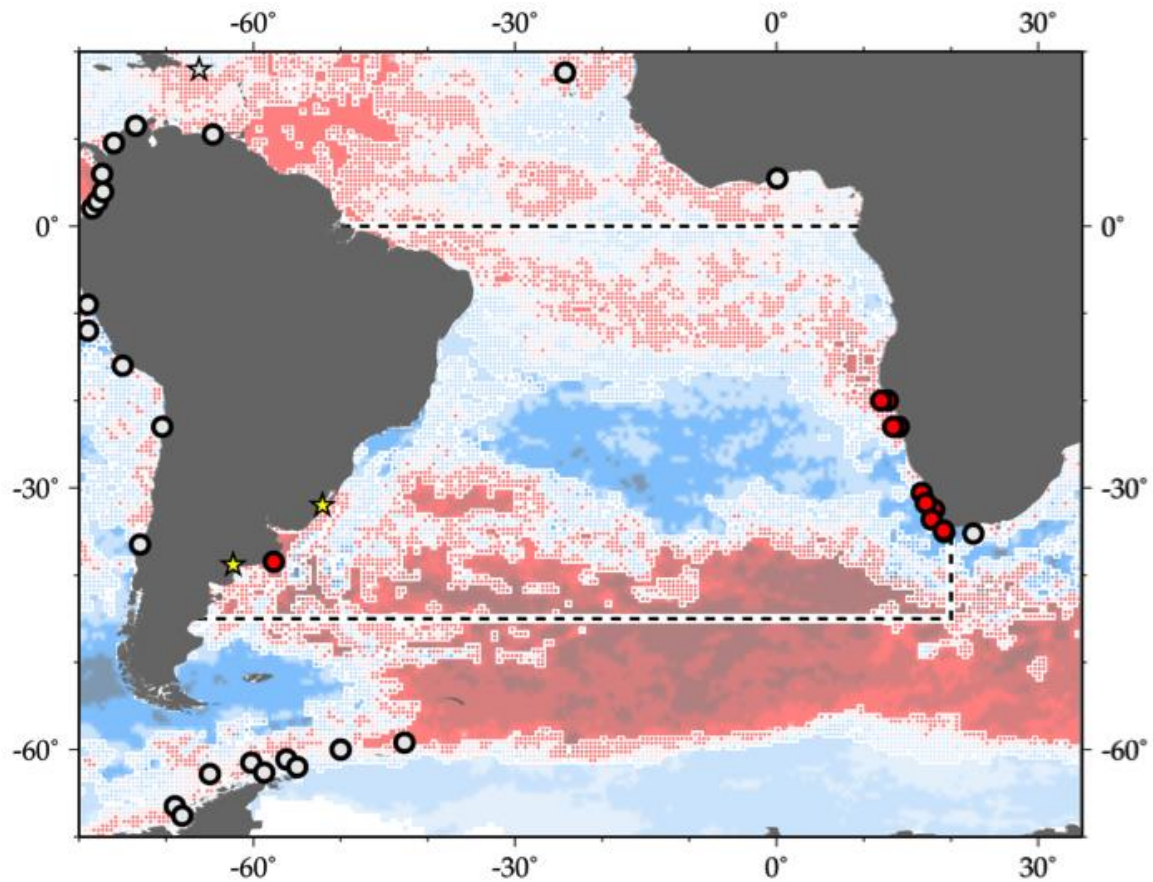


**Figure 5.1.** Map of IGMETS-participating South Atlantic time series on a background of a 10-year time-window (2003–2012) sea surface temperature trends (see also Figure 5.3). At the time of this report, the South Atlantic collection consisted of 13 time series (coloured symbols of any type), of which two were from estuarine areas (yellow stars). Dashed lines indicate boundaries between IGMETS regions. Uncoloured (gray) symbols indicate time series being addressed in a different regional chapter (e.g. Southern Ocean, South Pacific, North Atlantic). See Table 5.3 for a listing of this region’s participating sites. Additional information on the sites in this study is presented in the Annex.

## *Participating time-series investigators*

*Carla F. Berghoff, Mario O. Carignan, Fabienne Cazassus, Georgina Cepeda, Paulo Cesar Abreu, Rudi Cloete, Maria Constanza Hozbor, Daniel Cucchi Colleoni, Valeria Guinder, Richard Horaeb, Jenny Huggett, Anja Kreiner, Ezequiel Leonarduzzi, Vivian Lutz, Jorge Marcovecchio, Graciela N. Molinari, Nora Montoya, Ruben Negri, Clarisse Odebrecht, Luciano Padovani, Marcelo Pajaro, Andy Rees, M. Guillermina Ruiz, Valeria Segura, Ricardo I. Silva, Carla Spetter, Sakhile Tsotsobe, Marina Vera Diaz, Hans Verheye, and Maria Delia Viñas*

*This chapter should be cited as: Muller-Karger, F. E., Piola, A., Verheye, H.M., O'Brien, T. D., and Lorenzoni, L. 2017. South Atlantic Ocean. In What are Marine Ecological Time Series telling us about the ocean? A status report, pp. 83–96. Ed. by T. D. O'Brien, L. Lorenzoni, K. Isensee, and L. Valdés. IOC-UNESCO, IOC Technical Series, No. 129. 297 pp.*

## 5.1 Introduction

### 5.1.1 Geographic setting

The southern delimitation of the South Atlantic has been historically debated; oceanographically, the Subantarctic Front has been considered the southern limit of this ocean basin. The position of this front fluctuates between about 38°S and 58°S in the Atlantic. Here, we defined the South Atlantic as the area between the equator and 45°S and between the continental land masses of Africa and South America. Depending on this southern boundary delimitation, the South Atlantic covers an area of 30–40 million km<sup>2</sup> (ca. 10% of the total area of the world's oceans), with a volume of ca. 160 million km<sup>3</sup> (ca. 12% of the world's oceans volume) (Figure 5.1, Eakins and Sharman, 2010). It has an average depth of 3973 m and a maximum depth of 8240 m.

The South Atlantic started forming about 160 million years ago (late Jurassic and early Cretaceous) and is still spreading today. The western continental margins of the South Atlantic are broad between the equator, where the Amazon River discharges, and about 5°S (the bulge of Brazil). They become relatively narrow between this region and about 15°S. The margins become broader again to the south, with the Argentine (Patagonia) Shelf extending well over 400 km into the ocean, reaching around 850 km in width at about 50°S (Violante *et al.*, 2014). In the eastern South Atlantic, the broadest shelf is located off western South Africa around 29°S, becoming narrower in Namibia and to the north. Off the Congo River Delta, the shelf is only about 150 km wide and cut by a deep canyon (Savoie *et al.*, 2009).

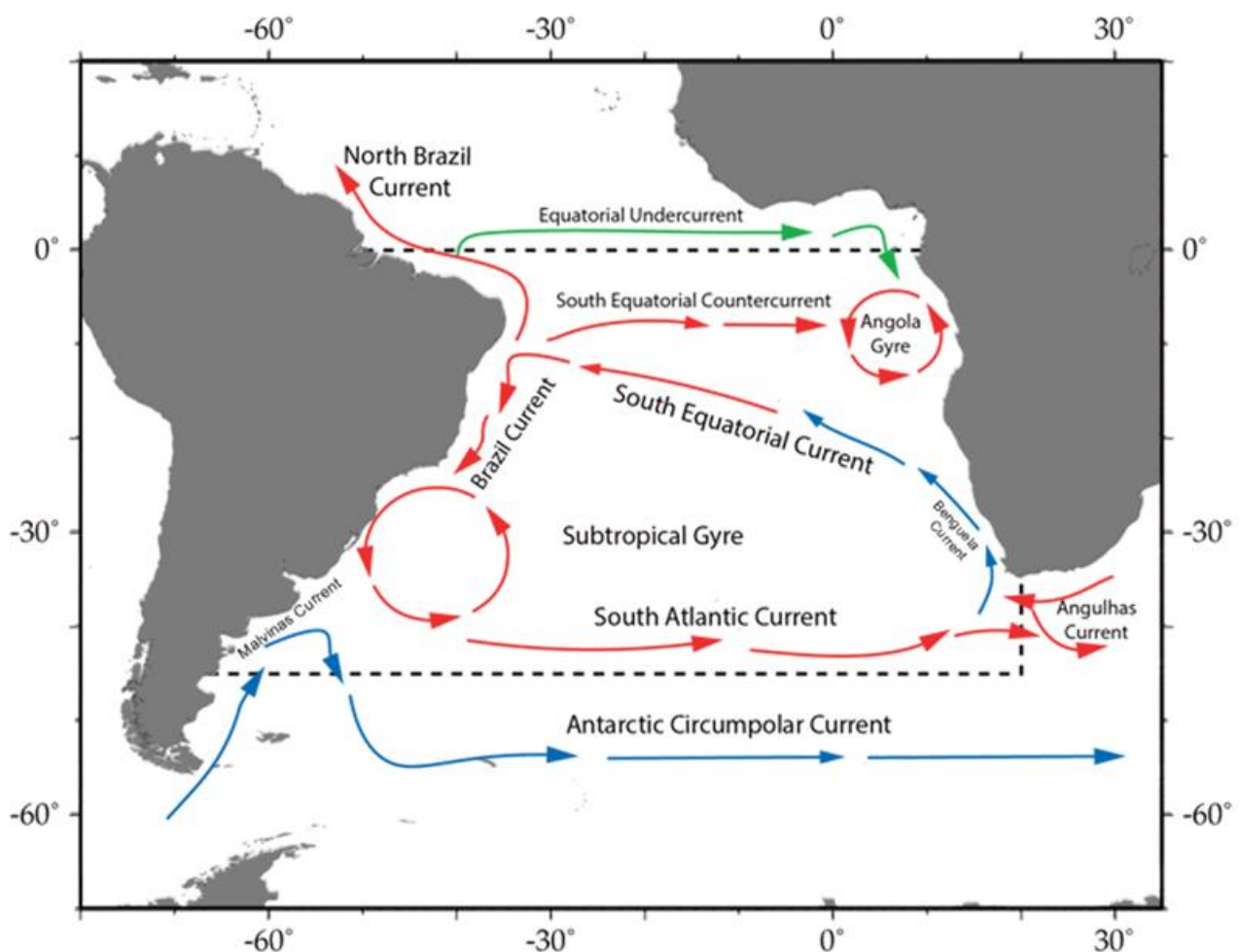


**Figure 5.2.** Schematic major current systems in the IGMETS-defined South Atlantic region. Red arrows indicate generally warmer water currents; blue arrows indicate generally cooler water currents.

### 5.1.2 Circulation patterns

The major physical oceanographic features of the South Atlantic have been described in numerous publications (Krummel, 1882; Deacon, 1933; Wefer *et al.*, 1996; Garzoli and Matano, 2011; and many others). Only a brief overview of the circulation that results from these forces is provided below for background.

The circulation of this basin is driven partly by winds and partly by the large-scale circulation that overturns the ocean over the scale of the entire Atlantic because of thermohaline imbalances. The atmosphere over the South Atlantic shows a high pressure system between Africa and South America, typically centred around 30°S. Toward the equator, the South Atlantic winds are dominated by the southeast trade winds. South of about 40°S there is a belt of prevailing westerlies that extends south over the Southern Ocean. Trade winds and the westerly wind belts define northern and southern regions, respectively, of the South Atlantic atmospheric high-pressure system. The region around 40°S, where the strong westerlies begin, represents a maximum in wind convergence (i.e. a maximum in Ekman forcing) in the South Atlantic. These patterns are strongly seasonal.

There is a net northward transport of heat from the South Atlantic to the North Atlantic across the equator. This significant cross-equatorial oceanic heat flux is characteristic in the Atlantic Ocean. Heat is carried north in surface layers of the South Atlantic via the southern branch of the South Equatorial Current, which originates with the Benguela Current in the southeastern Atlantic around 15–25°S off Africa (Figure 5.2). The current generally flows toward the northwest across the Atlantic and bifurcates in the central western portion of the Atlantic, with one branch going to the south/southwest (Brazil Current) and another going to the east/northeast merging into the North Brazil Current. This overall pattern is part of what is called the global Meridional Overturning Circulation (MOC; Lumpkin and Speer, 2007; Lopez *et al.*, 2016).

The South Atlantic is a mixing basin for many water masses that form in different parts of the world's oceans

(Garzoli and Matano, 2011). The South Atlantic gyre, centered approximately at 50°W and 30°S, is bound by a number of major surface ocean currents, including the Antarctic Circumpolar Current, the Benguela Current, the South Equatorial Current, the South Equatorial Counter Current, the Brazil Current, and the Malvinas (or Falkland) Current (Whitworth and Nowlin, 1987; Guhin *et al.*, 2003). There are strong variations in the Brazil and Malvinas (Falkland) currents and in the location and intensity of the Brazil/Malvinas Confluence in the western South Atlantic. These variations are important in defining the circulation, including the upwelling regime, and the biological productivity of the Patagonian Shelf (Matano *et al.*, 2010). Off South Africa, variation in the Agulhas Current and the Agulhas Retroflexion lead to variation in the Benguela Current. This is another important upwelling region in the South Atlantic (Andrews and Hutchings, 1980; Nelson and Hutchings, 1983; Shillington *et al.*, 2006). These changes, in turn, affect the northward flow of water across the South Atlantic that eventually crosses the equator into the North Atlantic.

The South Atlantic basin receives the discharge of many small rivers and some of the largest rivers of the world. These include the Congo-Chambeshi River and the Niger River off Africa and the Paraná-Rio de La Plata, Rio Negro, and São Francisco rivers off South America. The Amazon–Tocantins rivers discharge their water close to the equator off South America, but the majority of this water is advected northward toward the Caribbean Sea and toward the western North Atlantic (Müller-Karger *et al.*, 1988, 1995; Hu *et al.*, 2004; Johns *et al.*, 2014). Thus, it is not discussed in this chapter.

In the following sections, we summarize trends observed in ocean biogeochemistry time series for the South Atlantic region (Figure 5.1). The time series are discussed in the context of sea surface temperature (SST), sea surface chlorophyll concentration derived from satellites, and long-term gridded shipboard and model results for the South Atlantic for 1983–2012.

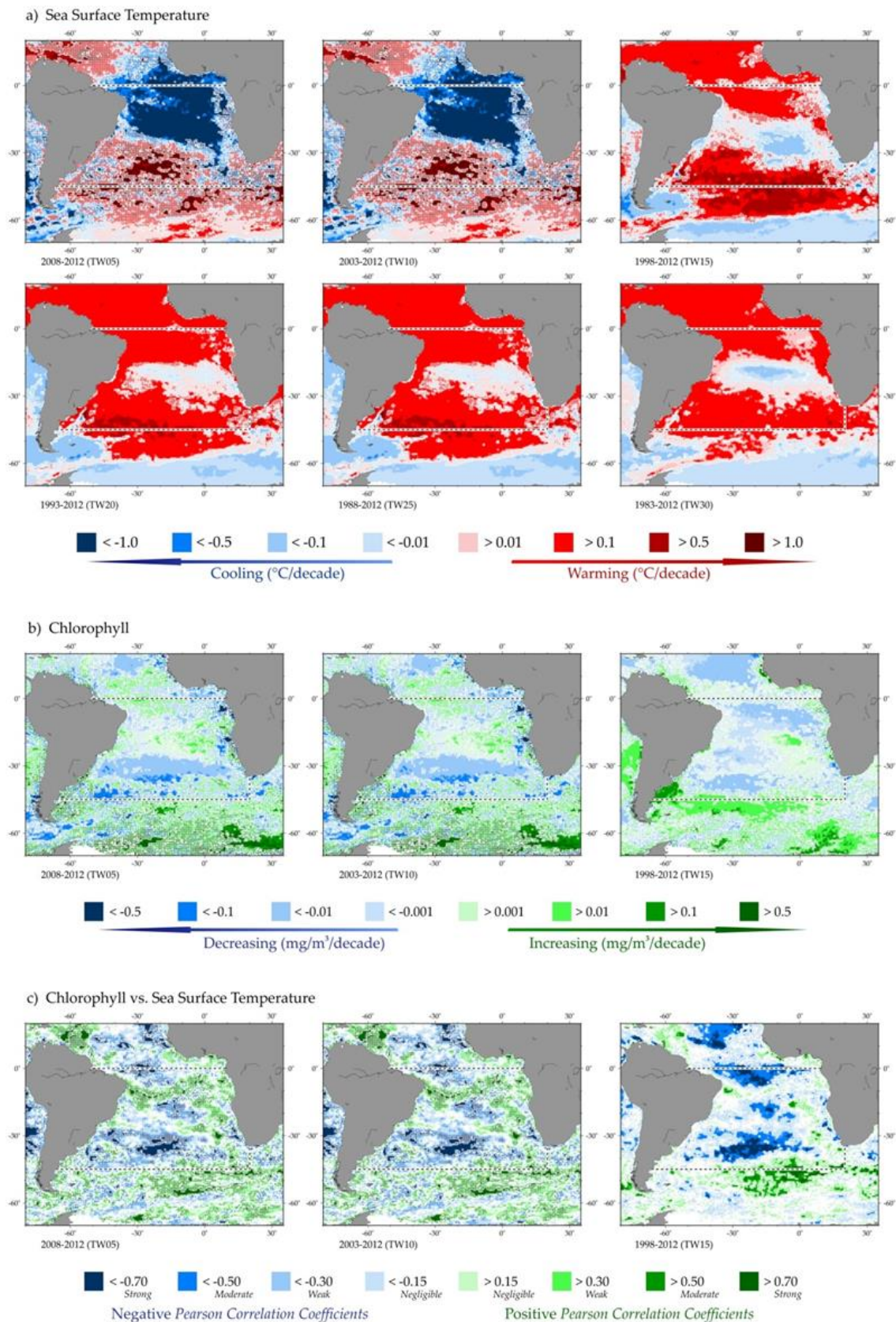


**Figure 5.3.** Annual trends in the South Atlantic sea surface temperature (a) and sea surface chlorophyll concentration (b), and correlations between chlorophyll and sea surface temperature (c) for each of the standard IGMETS time-windows. See “Methods” chapter for a complete description and methodology used.

## 5.2 General patterns of temperature and phytoplankton biomass

Different trends are described for particular variables over different time-frames. The reader is cautioned that changing the length of the time series examined will yield different trends. Some of the differences in the long-term trends examined may be due to shifts in the position of fronts and boundaries between water masses rather than changes within a single water mass. Such displacement in water masses can lead to an apparent increase or decrease in a property relative to conditions that may have prevailed in a particular region prior to such change.

The IGMETS time series of regional SST and satellite-derived chlorophyll *a* provide a means to assess change in the marine environment. Over the 30 years before 2012, nearly 86% of the South Atlantic warmed (75% at  $p < 0.05$ ; Figure 5.3; Table 5.1). However, the South Atlantic gyre featured a cooling trend. In contrast, over the more recent 10-year time-window (2003–2012), only about 45% of the South Atlantic showed warming and 55% showed cooling (Table 5.1). Even more recently, between 2008 and 2012, there was a large area between about 30°S and 10°N that showed cooling at 0.1°C year<sup>-1</sup>. Overall, 68% of the South Atlantic showed cooling during this period (Figure 5.3; Table 5.1). These results suggest that over the more recent 5- and 10-year time-periods, strong warming occurred primarily in temperate latitudes (i.e. south of ca. 30°S), with large areas showing >0.1°C year<sup>-1</sup> (or warming by ca. 1°C if extrapolated over a decade). The areas showing fastest warming south of the mid-ocean gyre are waters of the South Atlantic Current and of the Antarctic Circumpolar Current (Figures 5.3 and 5.2).

Trends of satellite-derived chlorophyll concentration showed significant increases in some areas over the different time-windows, but overall, chlorophyll decreased consistently over most of the South Atlantic between 1998 and 2012 (Table 5.2). A decrease in chlorophyll concentration of 0.001–0.01 mg m<sup>-3</sup> year<sup>-1</sup> was observed in the central gyre between the South Atlantic Current and the Benguela Current trends around 40°S over each of the time-periods examined (i.e. 2008–2012, 2003–2012, and 1998–2012). Much of this area experienced warming of >0.1°C year<sup>-1</sup> during these periods.

To the south near the boundary defined for the South Atlantic region, there was some increase in chlorophyll concentration between 1998 and 2012 in areas where

moderate warming was also observed. Concentrations increased considerably, particularly in the core of the Antarctic Circumpolar Current (Figures 5.3 and 5.2; Table 5.2; see also the “Southern Ocean” chapter, as these regions overlap). Indeed, over the 10-year time-window (2003–2012), most of the significant chlorophyll increase occurred south of 40°S (over 10% of the area of the basin; Table 5.2; Figure 5.3).

The fastest increase in chlorophyll in the South Atlantic occurred over the Patagonian Shelf, with rates >0.05 mg m<sup>-3</sup> year<sup>-1</sup> observed between 1998 and the early part of the 2000s. A large positive anomaly in chlorophyll concentration was observed in the composite between 1998 and 2003 and is driven by an intrusion of the Malvinas Current onto the shelf near 41°S in 2003 (Signorini *et al.*, 2009; Piola *et al.*, 2010). The analysis of the satellite-derived time series of chlorophyll concentration over the central area of the Patagonian Middle Shelf (around 40°S) by Delgado *et al.* (2015) shows that concentrations after 2003 and through 2010 were lower, with a decrease in the amplitude of the seasonal cycle.

Several large areas of high chlorophyll concentration and positive biomass trends corresponded to areas of high temperature and warming trends (Figure 5.3, lower panels). Such changes can be due to either increased stability in the water column (Signorini *et al.*, 2015), physiological changes in the phytoplankton and phytoplankton community composition changes over time (c.f. Behrenfeld *et al.*, 2015), a shift in the position of water masses, or a combination of these.

### 5.2.1 Potential correlations with climate indices

The North Atlantic Oscillation (NAO) tracks the difference between atmospheric pressures near Iceland and over the Azores. Fluctuations in the strength of these features change the jet stream, temperature, and precipitation in the North Atlantic. We examined whether there were correlations between chlorophyll concentration and the NAO in the South Atlantic over 5-, 10-, or 15-year periods. Overall, the spatial pattern of correlation between chlorophyll concentration and the NAO was patchy, and correlations were low. The only area where a spatially-coherent pattern emerged was in the central area of the South Atlantic along the Subantarctic Front. Here, significant inverse correlations were observed between chlorophyll concentration and the NAO.

**Table 5.1.** Relative spatial areas (% of the total region) and rates of change within within the South Atlantic region that are showing increasing or decreasing trends in sea surface temperature (SST) for each of the standard IGMETS time-windows. Numbers in brackets indicate the % area with significant ( $p < 0.05$ ) trends. See “Methods” chapter for a complete description and methodology used.

Latitude-adjusted SST data field surface area = 30.6 million km <sup>2</sup>	5-year (2008–2012)	10-year (2003–2012)	15-year (1998–2012)	20-year (1993–2012)	25-year (1988–2012)	30-year (1983–2012)
Area (%) w/ increasing SST trends ( $p < 0.05$ )	32.0% (10.7%)	44.9% (17.4%)	71.8% (45.9%)	90.5% (70.2%)	91.0% (74.2%)	85.7% (75.3%)
Area (%) w/ decreasing SST trends ( $p < 0.05$ )	68.0% (45.5%)	55.1% (26.2%)	28.2% (9.2%)	9.5% (0.5%)	9.0% (0.4%)	14.3% (6.6%)
> 1.0°C decade <sup>-1</sup> warming ( $p < 0.05$ )	12.5% (8.3%)	5.4% (5.4%)	0.7% (0.7%)	0.1% (0.1%)	0.0% (0.0%)	0.0% (0.0%)
0.5 to 1.0°C decade <sup>-1</sup> warming ( $p < 0.05$ )	9.6% (2.1%)	8.3% (6.8%)	12.2% (12.0%)	4.8% (4.8%)	0.7% (0.7%)	0.5% (0.5%)
0.1 to 0.5°C decade <sup>-1</sup> warming ( $p < 0.05$ )	7.8% (0.3%)	20.7% (5.2%)	43.9% (32.5%)	67.4% (61.7%)	66.9% (65.4%)	59.1% (58.9%)
0.0 to 0.1°C decade <sup>-1</sup> warming ( $p < 0.05$ )	2.1% (0.0%)	10.4% (0.1%)	15.0% (0.7%)	18.3% (3.6%)	23.3% (8.1%)	26.1% (15.9%)
0.0 to -0.1°C decade <sup>-1</sup> cooling ( $p < 0.05$ )	2.0% (0.0%)	10.3% (0.0%)	13.6% (0.5%)	8.5% (0.1%)	8.7% (0.2%)	11.9% (4.2%)
-0.1 to -0.5°C decade <sup>-1</sup> cooling ( $p < 0.05$ )	9.5% (0.6%)	30.7% (12.9%)	14.3% (8.5%)	0.9% (0.4%)	0.3% (0.2%)	2.4% (2.4%)
-0.5 to -1.0°C decade <sup>-1</sup> cooling ( $p < 0.05$ )	16.3% (8.7%)	13.6% (12.9%)	0.3% (0.2%)	0.1% (0.1%)	0.0% (0.0%)	0.0% (0.0%)
> -1.0°C decade <sup>-1</sup> cooling ( $p < 0.05$ )	40.2% (36.2%)	0.5% (0.4%)	0.0% (0.0%)	0.0% (0.0%)	0.0% (0.0%)	0.0% (0.0%)

Most of the South Atlantic SST showed low correlations with the NAO except for tropical and subtropical waters of the western Atlantic around the bulge of Brazil and southeastern South America to ca. 30°S in the area of the southern branch of the Brazil Current, with an inverse correlation with the NAO ( $p < -0.40$ ). This pattern is part of the spatial patterns of correlation observed over much of the tropical and subtropical North Atlantic.

During a positive NAO, there is a strengthening of the Icelandic low and Azores high. This strengthening results in an increased pressure gradient over the North Atlantic, which causes westerlies to increase in strength and cold air to move off the North American continent onto the ocean. Thus, when the NAO is positive, the North Atlantic and the tropical and subtropical South Atlantic tend to cool down, and when the NAO is negative, these areas warm up.

Another climate index is the Southern Oscillation Index (SOI). The SOI is based on the sea level atmospheric pressure differences between Tahiti and Darwin,

Australia. It is a measure of the differences in the atmosphere between the western and eastern tropical Pacific and tracks El Niño and La Niña episodes. Negative SOI values typically coincide with abnormally warm ocean waters across the eastern tropical Pacific, which is a characteristic of El Niño episodes. When the SOI is positive, colder waters typically occur across the eastern tropical Pacific (a characteristic of La Niña).

SST in tropical areas of the South Atlantic outside of, but adjacent to, the equatorial upwelling areas were strongly positively correlated with the SOI. Another area of positive correlation between SST and the SOI was the southern South Atlantic, south of the Subantarctic Front, i.e. in the Antarctic Circumpolar Current. SST of the central gyre of the South Atlantic showed a significant strong negative correlation with the SOI. In the central gyre, there were also areas of coherent positive correlations between chlorophyll and the SOI ( $p = 0.3-0.7$ ). These occurred mostly in an approximately 10° × 10° area centred around 30°S and 15°W and in a

20° wide band that occupied most of the Patagonia Shelf and extended east toward Africa along about 50°S. Everywhere else, correlations between chlorophyll and the SOI were poor, including in the tropical and central South Atlantic.

### 5.3 Trends from *in situ* time series

There are very few *in situ* oceanographic time series of biological, ecological, and biogeochemical observations in this part of the world's oceans (Figures 5.1 and 5.4). Most *in situ* observations in the South Atlantic have been collected either once at particular locations or over short periods. Most sampling programmes are not designed to

examine changes in time. One station that provides longer-term (15 years), comprehensive *in situ* measurements in the coastal marine environment is located on the Argentinian coast near Mar de Plata (Station EPEA). Another time series is located in Bahia Blanca, Argentina (1974–2016; Popovich *et al.*, 2008; Arias *et al.*, 2012; Spetter *et al.*, 2015).

The Patos Lagoon and estuary have time series from inland sites with temperature, salinity, and chlorophyll observations since 1993 (Abreu *et al.*, 2010; Odebrecht *et al.*, 2010; Haraguchi *et al.*, 2015). Since this summary chapter focuses on coastal and marine environments of the South Atlantic, the estuarine data are not discussed here.

**Table 5.2** Relative spatial areas (% of the total region) and rates of change within the South Atlantic region that are showing increasing or decreasing trends in phytoplankton biomass (CHL) for each of the standard IGMETS time-windows. Numbers in brackets indicate the % area with significant ( $p < 0.05$ ) trends. See “Methods” chapter for a complete description and methodology used.

Latitude-adjusted CHL data field surface area = 30.6 million km <sup>2</sup>	5-year (2008–2012)	10-year (2003–2012)	15-year (1998–2012)
Area (%) w/ increasing CHL trends ( $p < 0.05$ )	33.5% (5.5%)	38.9% (10.1%)	31.1% (10.9%)
Area (%) w/ decreasing CHL trends ( $p < 0.05$ )	66.5% (31.4%)	61.1% (28.5%)	68.9% (42.4%)
> 0.50 mg m <sup>-3</sup> decade <sup>-1</sup> increasing ( $p < 0.05$ )	1.3% (0.6%)	0.4% (0.2%)	0.6% (0.5%)
0.10 to 0.50 mg m <sup>-3</sup> decade <sup>-1</sup> increasing ( $p < 0.05$ )	3.0% (0.8%)	2.8% (1.7%)	3.4% (2.7%)
0.01 to 0.10 mg m <sup>-3</sup> decade <sup>-1</sup> increasing ( $p < 0.05$ )	17.4% (3.5%)	15.0% (6.0%)	9.9% (4.9%)
0.00 to 0.01 mg m <sup>-3</sup> decade <sup>-1</sup> increasing ( $p < 0.05$ )	12.0% (0.7%)	20.8% (2.1%)	17.2% (2.8%)
0.00 to -0.01 mg m <sup>-3</sup> decade <sup>-1</sup> decreasing ( $p < 0.05$ )	10.9% (1.1%)	26.6% (8.0%)	37.8% (20.1%)
-0.01 to -0.10 mg m <sup>-3</sup> decade <sup>-1</sup> decreasing ( $p < 0.05$ )	41.2% (21.3%)	30.3% (17.7%)	30.3% (21.8%)
-0.10 to -0.5 mg m <sup>-3</sup> decade <sup>-1</sup> (decreasing) ( $p < 0.05$ )	12.0% (7.4%)	3.4% (2.3%)	0.8% (0.5%)
> -0.50 mg m <sup>-3</sup> decade <sup>-1</sup> (decreasing) ( $p < 0.05$ )	2.4% (1.5%)	0.8% (0.5%)	0.0% (0.0%)

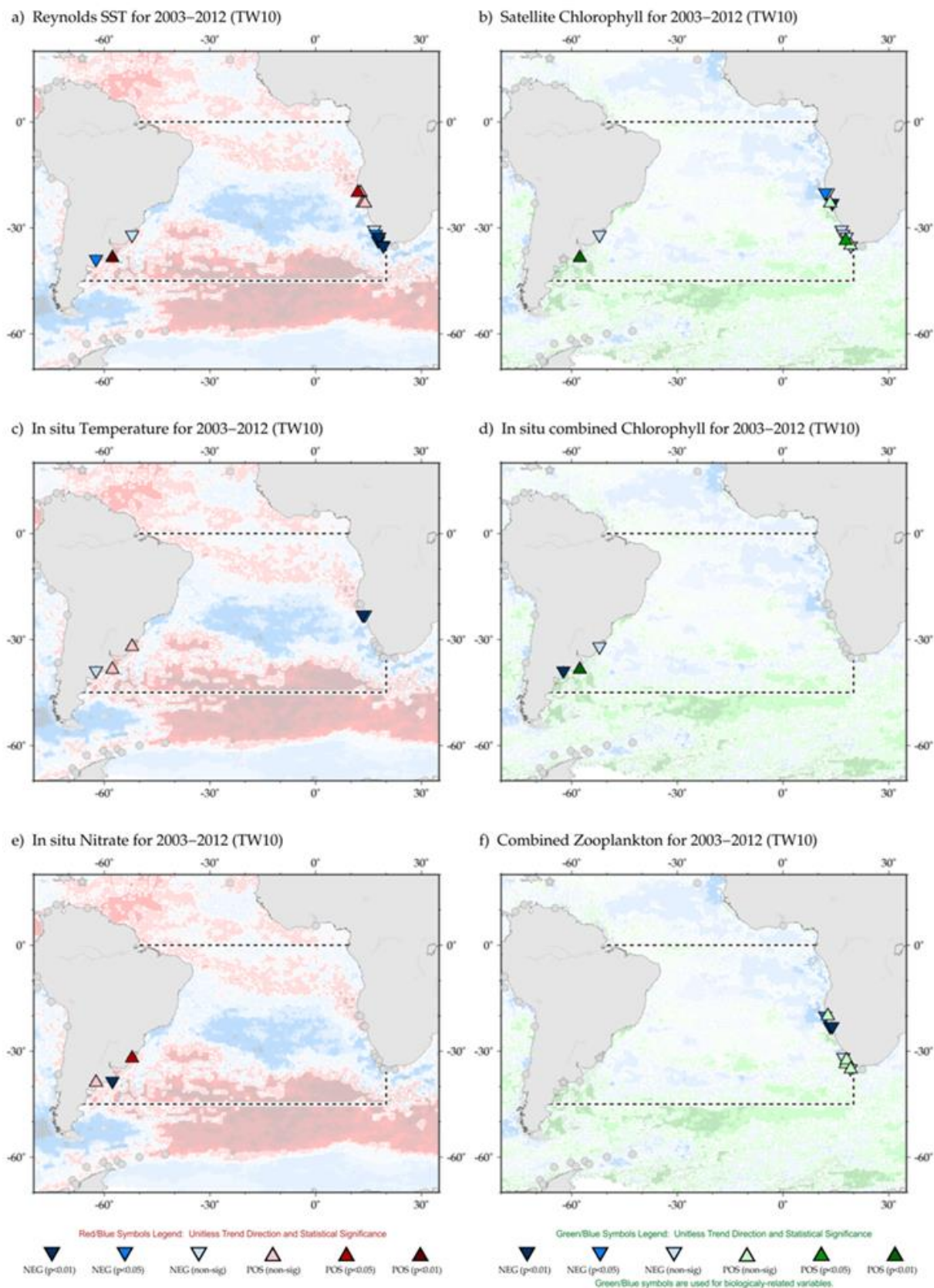


**Figure 5.4.** Map of South Atlantic region time-series locations and trends for select variables and IGMETS time-windows. Upward-pointing triangles indicate positive trends; downward triangles indicate negative trends. Gray circles indicate time-series site that fell outside of the current study region or time-window. Additional variables and time-windows are available through the IGMETS Explorer (<http://IGMETS.net/explorer>). See “Methods” chapter for a complete description and methodology used.

Along the southwestern coast of Africa, zooplankton measurements are intermittently available for the past 30 years (zooplankton and chlorophyll *a* time-series data are available from Walvis Bay off Namibia at 23°S; zooplankton data are available from Palgrave Point at 20°S off Namibia and various stations off South Africa). We present a summary of the trends observed with some of these time-series stations, but it is unfortunately impossible to extrapolate these trends to other regions of the central South Atlantic or to coastal areas removed from these locations.

The EPEA *in situ* chlorophyll time series shows a significant ( $p < 0.01$ ) increase in chlorophyll concentration during 2003–2012. The trend is not significant for the 15-year period 1998–2012 nor for the 5-year period spanning 2008–2012; the increase was, however, still visible. These observations are inconsistent with the satellite data over the middle shelf (Signorini *et al.*, 2009; Piola *et al.*, 2010), but they are consistent with satellite observations over the inner shelf (Delgado *et al.*, 2015). EPEA also reported increasing salinity and decreasing nitrate concentrations during this period. The trends remained consistent regardless of the time-window examined (5, 10, or 15 years; Figure 5.4).

In the northern Benguela, the *in situ* integrated (0–30 m) chlorophyll *a* concentration time series (2001–2012) off Walvis Bay showed a decline during 2001–2006, followed by an increase with peak values during 2009–2011. This is in contrast to the satellite-derived time series (1998–2012), which suggests an increase in surface chlorophyll *a* concentration since 2003. This is contrary to what would be expected from increasing SST associated with decreasing upwelling (Jarre *et al.*, 2015). There is no comparable uninterrupted, long-term, *in situ* chlorophyll *a* concentration time series for the southern Benguela. However, the phytoplankton data from ship (1980–2007) and satellite observations (1998–2012) indicate multiannual variability and a seasonal cycle, with very high concentrations due to dinoflagellate blooms in late local summer/autumn.

Again, there is also no obvious overall decade-scale trend in chlorophyll concentration (Hutchings *et al.*, 2009; Jarre *et al.*, 2015; Verheye *et al.*, 2016).

There have been long-term shifts in the abundance, biomass, production, and community structure (species and size composition) of zooplankton, and specifically copepods, in both the northern and southern Benguela over the past six decades (Verheye *et al.*, 2016). Copepods had been increasing in abundance since the

1950s. However, there was a turning point in the mid-1990s in the south and also in the mid-2000s in the north, after which zooplankton seemed to decline or stabilize. Indeed, a declining trend in copepod abundance was observed off the coast of Namibia and South Africa from the 1990s until the early-mid 2000's (15- and 20-year time windows). Conversely, over shorter 10- and 5-year time-windows, copepod abundance shows an increase again in those locations. A shift from large to smaller species dominating the copepod communities was observed in both Benguela subsystems. In the southern Benguela, copepod biomass and daily production were higher in the north (North and Central West Coast) than in the south (Southwest Coast and Western Agulhas Bank). They were higher in late local spring/early summer than in late autumn/early winter (Huggett *et al.*, 2009). Species and size composition of the copepod community also varied both spatially and seasonally.

Copepod biomass on the Western Agulhas Bank has declined by about 22% since 1988. In particular, the abundance of the large calanoid copepod *Calanus agulhensis* decreased by 44% (Jenny Huggett, pers. comm). This could be due to predation from an increase in pelagic fish biomass as well as an increase in SST. Marked declines in copepod biomass have also been observed on the Agulhas Bank off Mossel Bay, which falls within the Indian Ocean region (see Chapter 7).

## 5.4 Consistency with previous analyses

Several studies have described the general biogeography of the surface South Atlantic in terms of basic oceanographic characteristics (bathymetry, hydrography, productivity, and trophic structure). The most notable are the descriptions provided by Longhurst (1998, 2007) and those under the Large Marine Ecosystems (LME) classification (see summary in Sherman, 1991). Here, we provide a brief summary of major characteristics of marine ecosystems in the context of hydrology and chlorophyll concentration in the South Atlantic and how they compare with results from the observations presented here.

Sherman *et al.* (2009) point out that all of the LMEs of the world except for two (the California Current and Humboldt Current, both in the Eastern Pacific Ocean) showed warming between 1982 and 2006. In the South Atlantic, the temperature in tropical and subtropical LMEs rose 0.3–0.6°C during this period, while more temperate LMEs farther south warmed by <0.1°C. Fisheries yields in the Patagonian Shelf LME increased

over this period, while declining over the East and South Brazil Shelf LME (Müller-Karger *et al.*, 2017). Trends in these areas are likely due to high levels of fisheries exploitation rather than oceanographic or climate-related bottom-up controls (Sherman *et al.*, 2009). The Benguela Current LME off southwest Africa showed a declining trend in fisheries yields due to both heavy exploitation and environmental controls (van der Lingen *et al.*, 2006; Travers-Trolet *et al.*, 2014). Gherardi *et al.* (2010) attempted to examine large-scale drivers, including El-Niño Southern Oscillation (ENSO) and the Pacific Decadal Oscillation (PDO), and concluded that the features that defined the original LME will evolve with climate change, leading to possible changes in the core ecological criteria used to define these areas.

Similar to what was observed in this analysis, Signorini *et al.* (2015) found that the South Atlantic gyre, centred around 50°W and 30°S, showed a slight, but not significant, negative trend in chlorophyll concentration. This result covered a 16-year (1998–2013) record of combined SeaWiFS and MODIS chlorophyll *a* data, SST, and other complementary data. Vantrepotte and Mélin (2011) also found a decreasing trend in chlorophyll *a* concentration of ca.  $-1$  to  $-3\%$  year<sup>-1</sup> in the core of the South Atlantic gyre using a 10-year time series of SeaWiFS data (1997–2007). Polovina *et al.* (2008) had earlier suggested that there was both a negative trend in chlorophyll concentration as well as an expansion in the surface area occupied by low concentrations in the South Atlantic gyre area. However, the analysis by Gregg and Rousseux (2014) did not find a significant negative trend or an expansion of the area of low concentration in the South Atlantic gyre region using satellite chlorophyll time series spanning 1998–2012.

Consistent with the observations presented here, these prior studies also showed an increasing trend ( $>3\%$  year<sup>-1</sup>) in chlorophyll concentration in a broad band that traces the Benguela–South Equatorial Current, i.e. extending from southwest Africa to the bulge of Brazil in the eastern tropical South Atlantic. This increase is to the east and northeast of the South Atlantic gyre. The positive trend in chlorophyll *a* concentration along the edge of the Patagonian Shelf and extending across the southern South Atlantic basin just south of 45°S, i.e. in the area of the Subantarctic Front, was also reported in all these previous studies. As discussed earlier, changes in chlorophyll concentration on and along the mid- and outer Patagonian Shelf were related to changes in the physical structure of waters over the shelf and adjacent areas (Saraceno *et al.*, 2005; Romero *et al.*, 2006; Machado *et al.*, 2013; Valla and Piola, 2015).

Signorini *et al.* (2015) showed that the seasonal dynamics of chlorophyll concentration in the major ocean gyres, including the South Atlantic gyre, are closely tied to the depth of the mixed layer. In all basins, the seasonal chlorophyll peak coincided with the deepest mixed-layer depth. The analysis of satellite-derived chlorophyll *a* concentration and numerical model results of the South Atlantic basin by da Silveira Pereira *et al.* (2014) showed that chlorophyll and physical parameters, including surface temperature and salinity, exhibited correlations at zero lag, but also at frequencies that coincide with ENSO signals throughout the interior of the South Atlantic.

The eastern South Atlantic showed very dynamic oceanographic features. Rings (large eddies), shed periodically from the Agulhas Current, move to the northwest into the interior of the South Atlantic (see summary by Villar *et al.*, 2015). Agulhas rings, as well as Agulhas filaments and cyclonic eddies, interact with the shelf ecosystem. This exports large volumes of water and biological material (phytoplankton, zooplankton, and fish, fish eggs, and larvae) from the Agulhas Bank to the open ocean in the Indian Ocean, and far into the Atlantic Ocean (Duncombe Rae, 1991; Duncombe Rae *et al.*, 1992; Hutchings *et al.*, 1998).

## 5.5 Conclusions

In general, in the 5-year period prior to 2012, over 30% of the area of the South Atlantic showed warming, with nearly 70% of the area showing cooling (Table 5.1). However, when considering the two to three decades prior to 2012, nearly 90% of the area of the South Atlantic showed warming, with only about 10% showing no change or slightly decreasing SST trends (Table 5.1). About 30% of the area of the South Atlantic showed increasing chlorophyll *a* concentrations in the 5-year period prior to 2012, with over 66% of the area showing decreasing concentrations. The trends over the decade and a half spanning 1998–2012 were similar (Table 5.2).

The paucity of *in situ* time series in this region and the striking changes that have been reported in South Atlantic ecosystems over the past two decades highlight the need to have a better observing system in place. Such an observing system is needed to collect concurrent time series of physical, ecological, and biogeochemical observations.

**Table 5.3.** Time-series sites located in the IGMETS South Atlantic region. Participating countries: Argentina (ar), Brazil (br), Namibia (na), United Kingdom, (uk), and South Africa (za). Year-spans in red text indicate time series of unknown or discontinued status. IGMETS-IDs in red text indicate time series without a description entry in this Annex.

No.	IGMETS-ID	Site or programme name	Year-span	T	S	Oxy	Ntr	Chl	Mic	Phy	Zoo
1	<a href="#">ar-10101</a>	Puerto Cuatrerros (Bahia Blanca Estuary)	1975– present	X	X	X	X	X	-	-	-
2	<a href="#">ar-10201</a>	EPEA – Estacion Permanente de Estudios Ambientales (Argentine Coastal Waters)	2000– present	X	X	-	X	X	X	-	-
3	<a href="#">br-10101</a>	Patos Lagoon Estuary – Phytoplankton Time Series (Southeastern Brazil)	1993– present	X	X	-	X	X	X	X	-
4	<a href="#">na-10101</a>	Walvis Bay 23S shelf (Northern Benguela Current)	1978– present	X	X	X	-	-	-	-	X
5	<a href="#">na-10102</a>	Namibia 20S shelf (Northern Benguela Current)	2002– present	-	-	-	-	-	-	-	X
6	<a href="#">na-10103</a>	Walvis Bay 23S offshore (Northern Benguela Current)	1978– present	X	X	X	-	-	-	-	X
7	<a href="#">na-10104</a>	Namibia 20S offshore (Northern Benguela Current)	2002– present	-	-	-	-	-	-	-	X
8	<a href="#">uk-30601</a>	Atlantic Meridional Transect (AMT)	1995– present	X	X	X	X	X		X	X
9	<a href="#">za-10101</a>	St Helena Bay (Southern Benguela Current)	1951– present	X	X	-	-	-	-	-	X
10	<a href="#">za-30101</a>	SBCTS-A: North West Coast (Southern Benguela Current)	1988– present	-	-	-	-	-	-	-	X
11	<a href="#">za-30102</a>	SBCTS-B: Central West Coast (Southern Benguela Current)	1988– present	-	-	-	-	-	-	-	X
11	<a href="#">za-30103</a>	SBCTS-C: South West Coast (Southern Benguela Current)	1988– present	-	-	-	-	-	-	-	X
12	<a href="#">za-30104</a>	SBCTS-D: Western Agulhas Bank (Southern Benguela Current)	1988– present	-	-	-	-	-	-	-	X
13	<a href="#">za-30201</a>	ABCTS Danger Point Monitoring Line (Agulhas Bank)	1988– present	-	-	-	-	-	-	-	X

## 5.6 References

- Abreu, P. C., Bergesch, M., Proença, L. A., Garcia, C. A. E., and Odebrecht, C. 2010. Short- and long-term chlorophyll a variability in the shallow microtidal Patos Lagoon Estuary, Southern Brazil. *Estuaries and Coasts*, 33: 554–569, doi:10.1007/s12237-009-9181-9.
- Andrews, W. R. H., and Hutchings, L. 1980. Upwelling in the Southern Benguela Current. *Progress in Oceanography*, 9(1): 1–81, doi:10.1016/0079-6611(80)90015-4.
- Arias, A. H., Piccolo, M. C., Spetter, C. V., Freije, R. H., and Marcovecchio, J. E. 2012. Lessons from multi-decadal oceanographic monitoring at an estuarine ecosystem in Argentina. *International Journal of Environmental Research*, 6(1): 219–234.
- Behrenfeld, M. J., O'Malley, R. T., Boss, E. S., Westberry, T. K., Graff, J. R., Halsey, K. H., Milligan, A. J., *et al.* 2015. Revaluating ocean warming impacts on global phytoplankton. *Nature Climate Change*, 5: doi:10.1038/NCLIMATE2838.
- Deacon, G. E. R. 1933. A general account of the hydrology of the South Atlantic Ocean. *Discovery Reports*, 7: 171–238.
- da Silveira Pereira, N. E., Harari, J., and de Camargo, R. 2014. Correlations of remote sensing chlorophyll-a data and results of a numerical model of the tropical and South Atlantic Ocean circulation. *Journal of Geology and Geosciences*, 3: 171, doi:10.4172/2329-6755.1000171.
- Delgado, A. L., Loisel, H., Jamet, C., Vantrepotte, V., Perillo, G. M. E., and Piccolo, M. C. 2015. Seasonal and inter-annual analysis of chlorophyll-a and inherent optical properties from satellite observations in the inner and mid-shelves of the south of Buenos Aires Province (Argentina). *Remote Sensing*, 7: 11821–11847, doi:10.3390/rs70911821.
- Duncombe Rae, C. M. 1991. Agulhas retroflection rings in the South Atlantic: an overview. *South African Journal of Marine Science*, 11: 327–344.
- Duncombe Rae, C. M., Shillington, F., Agenbag, J., Taunton-Clark, J., and Grundlingh, M. 1992. An Agulhas ring in the South Atlantic ocean and its interaction with the Benguela upwelling frontal system. *Deep-Sea Research*, 39: 2009–2027.
- Eakins, B. W., and Sharman, F. 2010. Volumes of the World's Oceans from ETOPO1. NOAA National Geophysical Data Center, Boulder, CO.
- Garzoli, S. L., and Matano, R. 2011. The South Atlantic and the Atlantic meridional overturning circulation. *Deep-Sea Research II*, 58(17–18): 1837–1847, doi:10.1016/j.dsr2.2010.10.063.
- Gherardi, D. F. M., Tavares Paes, E., Cahanhuk Soares, H., Ponzi Pezzi, L., and Kayano, M. T. 2010. Differences between spatial patterns of climate variability and large marine ecosystems in the western South Atlantic. *Pan-American Journal of Aquatic Sciences*, 5(2): 310–319.
- Gregg, W. W., and Rousseaux, C. S. 2014. Decadal trends in global pelagic ocean chlorophyll: A new assessment integrating multiple satellites, in situ data, and models, *Journal of Geophysical Research Oceans*, 119: 5921–5933, doi:10.1002/2014JC010158.
- Guhin, S., Ray, P., Mariano, A. J., and Ryan, E. H. 2003. The South Atlantic Current. *Ocean Surface Currents*. <http://oceancurrents.rsmas.miami.edu/southern/south-atlantic.html>.
- Haraguchi, L., Carstensen, J., Abreu, P. C., and Odebrecht, C. 2015. Long-term changes of the phytoplankton community and biomass in the subtropical shallow Patos Lagoon Estuary, Brazil. *Estuarine, Coastal and Shelf Science*, 162: 76–87.
- Huggett, J., Verheye, H., Escribano, R., and Fairweather, T. 2009. Copepod biomass, size composition and production in the Southern Benguela: Spatio-temporal patterns of variation, and comparison with other eastern boundary upwelling systems. *Progress in Oceanography*, 83(1): 197–207.
- Hutchings, L., Barange, M., Bloomer, S. F., Boyd, A. J., Crawford, R. J. M., Huggett, J. A., Kerstan, M., *et al.* 1998. Multiple factors affecting South African anchovy recruitment in the spawning, transport, and nursery areas. *In Benguela Dynamics: Impacts of Variability on Shelf-Sea Environments and their Living Resources*, pp. 211–225. Ed. by S. C. Pillar, C. L. Moloney, A. I. L. Payne, and F.A. Shillington. *South African Journal of Marine Science*, 19.

- Hutchings, L., van der Lingen, C. D., Shannon, L. J., Crawford, R. J. M., Verheye, H. M. S., Bartholomae, C. H., van der Plas, A. K., *et al.* 2009. The Benguela Current: An ecosystem of four components, *Progress in Oceanography*, 83: 15–32.
- Hu, C., Montgomery, E. T., Schmitt, R. W., and Muller-Karger, F. E. 2004. The Amazon and Orinoco River plumes in the tropical Atlantic and Caribbean Sea: Observation from space and S-PALACE floats. *Deep-Sea Research Part II. Topical Studies in Oceanography*, 51(10–11): 1151–1171.
- Jarre, A., Hutchings, L., Kirkman, S. P., Kreiner, A., Tchupalanga, P., Kainge, P., Uanivi, U., *et al.* 2015. Synthesis: climate effects on biodiversity, abundance and distribution of marine organisms in the Benguela. *Fisheries Oceanography*, 24 (Suppl. 1): S122–S149.
- Johns, E. M., Muhling, B. A., Perez, R. C., Müller-Karger, F. E., Melo, N., Smith, R. H., Lamkin, J. T., *et al.* 2014. Amazon River water in the northeastern Caribbean Sea and its effect on larval reef fish assemblages during April 2009. *Fisheries Oceanography*, 23: 472–494, doi:10.1111/fog.12082.
- Krummel, O. 1882: Bemerkungen über die Meeresströmungen und Temperaturen in der Falklandsee. Aus dem Archiv der Deutschen Seewarte, V(2). 25 pp.
- Longhurst, A. R. A. 1998. *Ecological Geography of the Sea*. Academic Press, San Diego. 398 pp.
- Longhurst, A. R. A. 2007. *Ecological Geography of the Sea*, 2nd edn. Academic Press, San Diego. 542 pp.
- Lopez, H., Dong, S., Lee, S-K., and Goni, G. 2016. Decadal modulations of interhemispheric global atmospheric circulations and monsoons by the South Atlantic Meridional Overturning Circulation. *Journal of Climate*, 29: 1831–1851, doi:http://dx.doi.org/10.1175/JCLI-D-15-0491.1.
- Lumpkin, R., and Speer, K. 2007. Global ocean meridional overturning. *Journal of Physical Oceanography*, 37: 2550–2562.
- Machado, I., Barreiro, M., and Calliari, D. 2013. Variability of chlorophyll-*a* in the Southwestern Atlantic from satellite images: Seasonal cycle and ENSO influences. *Continental Shelf Research*, 53: 102–109.
- Matano, R. P., Palma, E. D., and Piola, A. R. 2010. The influence of the Brazil and Malvinas Currents on the southwestern Atlantic shelf circulation. *Ocean Science*, 6: 983–995.
- Muller-Karger, F. E., McClain, C. R., and Richardson, P. L. 1988. The dispersal of the Amazon's water. *Nature*, 333: 56–59.
- Muller-Karger, F. E., Richardson, P. L., and McGillicuddy, D. 1995. On the offshore dispersal of the Amazon's Plume in the North Atlantic. *Deep-Sea Research I*, 42(11–12): 2127–2137.
- Muller-Karger, F., Rueda-Roa, D., Chavez, F., Kavanaugh, M., and Roffer, M. A. 2017. Megaregions among the Large Marine Ecosystems of the Americas. *Environmental Development*, <http://dx.doi.org/10.1016/j.envdev.2017.01.005>.
- Nelson, G., and Hutchings, L. 1983. The Benguela upwelling area. *Progress in Oceanography*, 12(3): 333–356.
- Odebrecht, C., Abreu, P. C., Bemvenuti, C. E., Copertino, M., Muelbert, J. H., Vieira, J. P., and Seeliger, U. 2010. The Patos Lagoon Estuary: Biotic responses to natural and anthropogenic impacts in the last decades (1979–2008). *In Coastal Lagoons: Critical Habitats of Environmental Change*, pp. 433–455. Ed. by M. J. Kennish, and H. W. Paerl. CRC Press, Boca Raton, FL. 568 pp.
- Piola, A. R., Martinez Avellaneda, N., Guerrero, R. A., Jardon, F. P., Palma, E. D., and Romero, S. I. 2010. Malvinas-slope water intrusions on the northern Patagonia continental shelf. *Ocean Science*, 6: 345–359.
- Polovina, J. J., Howell, E. A., and Abecassis, M. 2008. Ocean's least productive waters are expanding. *Geophysical Research Letters*, 35: L03618, doi:10.1029/2007GL031745.
- Popovich, C. A., Spetter, C. V., Marcovecchio, J. E., and Freije, R. H. 2008. Dissolved nutrient availability during winter diatom bloom in a turbid and shallow estuary (Bahia Blanca, Argentina). *Journal of Coastal Research*, 24(1): 95–102.
- Romero, S. I., Piola, A. R., Charo, M., and Garcia, C. A. E. 2006. Chlorophyll-*a* variability off Patagonia based on SeaWiFS data, *Journal of Geophysical Research*, 111: C05021, doi:10.1029/2005JC003244.

- Saraceno, M., Provost, C., and Piola, A. R. 2005. On the relationship between satellite-retrieved surface temperature fronts and chlorophyll a in the western South Atlantic. *Journal of Geophysical Research*, Oceans, 110(C11): doi:10.1029/2004JC002736.
- Savoie, B., Babonneau, N., Dennielou, B., and Bez, M. 2009. Geological overview of the Angola–Congo margin, the Congo deep-sea fan and its submarine valleys. *Deep-Sea Research Part II: Topical Studies in Oceanography*, 56(23): 2169–2182.
- Sherman, K. 1991. The Large Marine Ecosystem concept: research and management strategy for living marine resources. *Ecological Applications*, 1: 349–360, <http://dx.doi.org/10.2307/1941896>.
- Sherman, K., Belkin, I. M., Friedland, K. D., O'Reilly, J., and Hyde, K. 2009. Accelerated warming and emergent trends in fisheries biomass yields of the world's large marine ecosystems. *Ambio*, 4: 215–224.
- Shillington, F. A., Reason, C. J. C., Duncombe, C. M., Florenchie, R. P., and Penven, P. 2006. Large scale physical variability of the Benguela Current Large Marine Ecosystem (BCLME). *In* Large Marine Ecosystems, Vol. 14, pp. 47–68. Ed. by V. Shannon, G. Hempel, P. Malanotte-Rizzoli, C. Moloney, and J. Woods. Elsevier. 410 pp.
- Signorini, S. R., Franz, B. A., and McClain, C. R. 2015. Chlorophyll variability in the oligotrophic gyres: mechanisms, seasonality and trends. *Frontiers in Marine Science*, 02: <http://dx.doi.org/10.3389/fmars.2015.00001>.
- Signorini, S. R., Garcia, V. M. T., Piola, A. R., Evangelista, H., McClain, C. R., Garcia, C. A. E., and Mata, M. M. 2009. Further studies on the physical and biogeochemical causes for large interannual changes in the Patagonian Shelf spring-summer phytoplankton bloom biomass. NASA/TM-2009-214176, NASA Goddard Space Flight Center, Greenbelt, MD, USA.
- Spetter, C. A., Popovich, C. A., Arias, A., Asteasuain, R. O., Freije, R. H., and Marcovecchio, J. E. 2015. Role of nutrients in the phytoplankton development during a winter diatom bloom in a eutrophic South American estuary (Bahia Blanca, Argentina). *Journal of Coastal Research*, 31(1): 76–87.
- Travers-Trolet, M., Shin, Y.-J., Shannon, L. J., Moloney, C. L., and Field, J. G. 2014. Combined fishing and climate forcing in the Southern Benguela upwelling ecosystem: an end-to-end modelling approach reveals dampened effects. *PLOS ONE*, 9(4): e94286, doi:10.1371/journal.pone.0094286.
- Valla, D., and Piola, A. R. 2015. Evidence of upwelling events at the northern Patagonian shelf break. *Journal of Geophysical Research Oceans*, 120(11): 7635–7656, doi:10.1002/2015JC011002.
- van der Lingen, C., Freon, P., Hutchings, L., Roy, C., Bailey, G., Bartholomae, C., Cockcroft, A., *et al.* 2006. Resource and ecosystem variability, including regime shifts, in the Benguela Current system. *In* Benguela: Predicting a Large Marine Ecosystem, pp. 147–184. Ed. by V. Shannon, G. Hempel, P. Malanotte-Rizzoli, C. Moloney, and J. Woods. Elsevier. 438 pp.
- Vantrepotte, V., and Melin, F. 2011. Inter-annual variations in the SeaWiFS global chlorophyll *a* concentration (1997–2007). *Deep-Sea Research Part I*, 58: 429–441.
- Verheye, H., Lamont, T., Huggett, J. A., Kreiner, A., and Hampton, I. 2016. Plankton productivity of the Benguela Current Large Marine Ecosystem (BCLME). *Environmental Development*, 17: <http://dx.doi.org/10.1016/j.envdev.2015.07.011i>
- Villar, E, Farrant, G. K., Follows, M., Garczarek, L., Speich, S., Audic, S., Bittner, L., *et al.* 2015. Ocean plankton. Environmental characteristics of Agulhas rings affect inter-ocean plankton transport. *Science*, 348(6237): 1261447, doi:10.1126/science.1261447.
- Violante, R. A., Paterlini, C. M., Marcolini, S. I., Costa, I. P., Cavallotto, J. L., Laprida, C., Dragani, W., *et al.* 2014. The Argentine continental shelf: morphology, sediments, processes and evolution since the Last Glacial Maximum. *In* Continental Shelves of the World: Their Evolution During the Last Glacio-Eustatic Cycle, pp. 55–68. Ed. by F. L. Chiocci, and A. R. Chiva. Geological Society Memoir No. 41, The Geological Society, London. 343 pp.
- Wefer, G., Berger, W. H., Siedler, G., and Webb, D. J. 1996. *The South Atlantic: Present and Past Circulation*. Springer, Berlin Heidelberg. 644 pp.
- Whitworth, T., and Nowlin Jr., W. D. 1987. Water masses and currents of the southern ocean at the Greenwich meridian, *Journal of Geophysical Research*, 92: 6462–6476.